Photo-double detachment from the F⁻ ion

V T Davis[1]**, A Aguilar**[2]**, A M Covington**[2]**, J S Thompson**[2]**, D Calabrese**[3]**,
C Cisneros**[4]**, M S Gulley**[5]**, M Halka**[6]**, D Hanstorp**[7]**, J Sandström**[7]**,
B M McLaughlin**[8]**, G F Gribakin**[8] **and D J Pegg**[9]

[1] Department of Physics, United States Military Academy, West Point, NY 10996, USA
[2] Department of Physics and Chemical Physics Programme, University of Nevada, Reno,
Nevada 89557-0058, USA
[3] Department of Physics, Sierra College, Rocklin, CA 95677, USA
[4] Centro de Ciencias Físicas UNAM, Apdo. Postal 48-3 CP 62251 Cuernavaca, Mor. México
[5] LANCSE Division, Los Alamos National Laboratory, Los Alamos, NM 87545, USA
[6] Department of Physics, Embry-Riddle Aeronautical University, Prescott, AZ 86301, USA
[7] Department of Physics, Chalmers University of Technology and Göteborg University,
SE-412 96 Göteborg Sweden
[8] Department of Applied Mathematics and Theoretical Physics, Queens University,
Belfast BT7 1NN, UK
[9] Department of Physics, University of Tennessee, Knoxville, TN 37996, USA

Abstract

The correlated process of photodetaching two electrons from the F⁻ ion
following the absorption of a single photon has been investigated over an energy
range 20–62 eV. In the experiment, a beam of photons from the Advanced Light
Source was collinearly merged with a counter-propagating beam of F⁻ ions
from a sputter ion source. The F⁺ ions produced in the interaction region
were detected, and the normalized signal was used to monitor the relative cross
section for the double-detachment reaction. An absolute scale for the cross
section was established by measuring the spatial overlap of the two beams
and by determining the efficiency for collection and detection of the F⁺ ions.
The measured cross section is compared with R-matrix and random phase
approximation calculations. These calculations show that the Auger decay of
the $2s2p^6$ core-excited state of the F atom plays a minor role in the production of
F⁺ ions and that double detachment is likely to be dominated by simultaneous
correlated ejection of two valence electrons at energies well above threshold.

1. Introduction

The outermost electron in a negative ion is bound to the parent atom by a force due to
the short-range electrostatic interaction and the induced polarization of the atom by this
electron. Polarization involves correlations between the extra electron and the atomic electrons.
The stability of negative ions depends critically on the extent that the extra electron can

share the attractive field of the nucleus. Negative ions exhibit an enhanced sensitivity to electron correlation due to the fact that the inter-electronic interactions become relatively more important than the electron–nucleus interactions as a result of the efficient shielding of the nuclear charge by the atomic electrons. The weak and short-range polarization binding force in a negative ion results in a structure that is qualitatively different from that of an atom or positive ion [1]. Negative ions typically have only a single bound state in contrast to the infinite spectrum of bound states associated with an atom or positive ion. Loosely bound systems such as negative ions are well suited for studies of higher-order processes in the photon–ion interaction since energy exchanges are expected to be much smaller in comparison to those occurring in isoelectronic atoms and positive ions. The increasing availability of bright, highly collimated, high-energy synchrotron radiation sources over the past several years has made it possible to experimentally study the photo-detachment of more than one electron from a negative ion.

The subject of this paper is two-electron detachment from the F^- ion following the absorption of a single, high-energy photon. The F^- ion has a closed-shell ground state configuration of $1s^2 2s^2 2p^6$. As a result, the six valence electrons are relatively strongly bound and also strongly correlated. The electron affinity of the F atom was measured by Blondel *et al* [2] to be 3.4011895(25) eV. Due to this relatively large value, laser-based studies of F^- have primarily focused on multi-photon-induced detachment processes involving the use of two or more photons to detach a single valence electron. In this paper we have investigated another higher-order process, multiple electron detachment. Multiple detachment processes, in which two or more electrons are ejected from a negative ion following the absorption of a single photon, are expected to involve a significant amount of electron correlation. We report on a joint experimental and theoretical study of the cross section for production of F^+ ions from F^- ions over the photon energy range 20–62 eV. This range encompasses the double-detachment continuum from just above the threshold at the $F^+(2s^2 2p^4\ ^3P)$ limit up to the $F^{2+}(2s^2 3p^3\ ^4S_o)$ limit. The measurement of F^+ production relates directly to the cross section for photo-double detachment.

There have been several previous investigations of cross sections for photo-double detachment. Most of the studies, however, have focused on threshold behaviour or resonance structure in the detachment cross section. The first measurement of photo-double detachment was made by Donahue *et al* [3], who studied the threshold behaviour of the cross section for the detachment of both electrons from the H^- ion. Later, similar measurements were made on the metastable He^- ion by Bae *et al* [4] and the stable K^- ion by Bae and Peterson [5]. All three experiments employed lasers to directly detach a pair of valence electrons. More recently, synchrotron radiation has been used to investigate more energetic processes involving inner-shell excitation and detachment from negative ions. Kjeldsen *et al* [6], for example, reported the first measurement of a cross section for photo-double detachment over an extended energy range. In this experiment the cross section for the production of Li^+ ions following the absorption of a single photon by the Li^- ion was measured over the energy range 56–70 eV. The cross section measurement was absolute but the emphasis of the experiment was on the resonance structure in the cross section. The resonances in this case were associated with the autodetaching decay of K-shell core-excited states of Li^-. Similar studies on both the Li^- and He^- ions were made by Berrah *et al* [7, 8]. Gibson *et al* [9] have investigated K-shell excitation in C^-. Recently Bilodeau *et al* [10] reported on further investigations of the structure of the He^- ion. A review of the work of this research group has recently been published by Berrah *et al* [11]. The photo-double detachment cross section for the Na^- ion was measured by Covington *et al* [12] over a photon energy range 30–51 eV. Again, the cross section measurements were absolute but the focus of the work was on determining the

energies and widths of resonances in the cross section. In this case the observed resonances were associated with L-shell core-excited states of the Na$^-$ ion. Most recently, Aguilar *et al* [13] investigated the photo-double detachment cross section of Cl$^-$. Several theoretical treatments of photo-double detachment have emerged recently. For example, Zhou *et al* [14, 15]. Zatsarinny *et al* [16] and Carlin *et al* [17] have used *R*-matrix methods to calculate photodetachment cross sections of Li$^-$, He$^-$ and Be$^-$ at energies corresponding to K-shell excitations. Random phase approximation (RPA) calculations by Amusia *et al* [18] and Radojevic *et al* [19] determined cross sections for the production of inner-shell vacancies in the negative ions of the halogens. Such vacancies result in core-excited states of the atoms and lead to double detachment via the Auger effect, provided they lie above the positive ion threshold. In this paper the measured cross section is compared to that calculated using the *R*-matrix formalism. A new RPA calculation has also been made in order to try to understand the role played by the intermediate core excited $2s2p^6$ state of the F atom in the production of F$^+$ ions from F$^-$ ions.

2. Theory

In this section we consider possible mechanisms for either simultaneous or sequential detachment of two electrons from the F$^-$ ion following the absorption of a photon of energy in the energy range 20–62 eV. The double-detachment reaction can be written as

$$\gamma + \text{F}^-(i) \rightarrow \text{F}^+(j) + 2\,\text{e}^-. \tag{1}$$
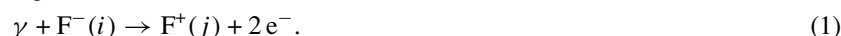
In the present experiment, we did not detect the ejected photoelectrons but rather the F$^+$ ions produced in the detachment process. The symbols (i) and (j) represent the internal energy states of the negative ion and atom, respectively. The initial state (i) is the $2s^22p^6\,^1\text{S}$ ground state of F$^-$, but the final state (j) may be the ground state or any excited state of F$^+$, depending on the energy of the absorbed photon. Over the range 20–62 eV, possible final state configurations of F$^+$ are $2s^22p^4$, $2s2p^5$, $2s^22p^3nl$, etc (throughout this paper the $1s^2$ core will be omitted from configuration labels since it is inert in the range of photon energies studied). The detection of the F$^+$ ions was nonselective with regard to their internal energy state. The data obtained in the experiment therefore represent the sum of all the partial cross sections associated with the different final states of F$^+$.

The double-detachment continuum, F$^+$ + 2e$^-$, representing the final state of the reaction shown in equation (1) has a threshold at 20.82 eV relative to the ground state of the F$^-$ ion. Figure 1 shows three possible photon-induced mechanisms in which two electrons are ejected from a F$^-$ ion, either simultaneously or sequentially, to form a F$^+$ ion. In the direct process, two 2p electrons are simultaneously ejected from the outer or valence shell. Since the electric dipole operator is a single-electron operator, this process would involve correlation between the valence electrons. In the energy range of the present experiment, the simplest indirect process would be initiated by the detachment of a 2s inner-shell electron. The vacancy in the 2s sub-shell of F could then be filled by Auger decay as a 2p electrons drops into the 2s hole, resulting in the detachment of a 2p outer shell electron. This sequential process involves intermediate core-excited states of F that would have to lie above the threshold of the double-detachment continuum at 20.82 eV. The sequential two-step Auger process can be written as

$$\gamma + \text{F}^-(i) \rightarrow \text{F}^{**}(j) + \text{e}^- \tag{2}$$
$$\text{F}^{**}(j) \rightarrow \text{F}^+(k) + \text{e}^-. \tag{3}$$

In the above reactions the symbols (i), (j) and (k) represent internal energy states of the negative ion, core-excited atom and positive ion, respectively. The state (i) is again the
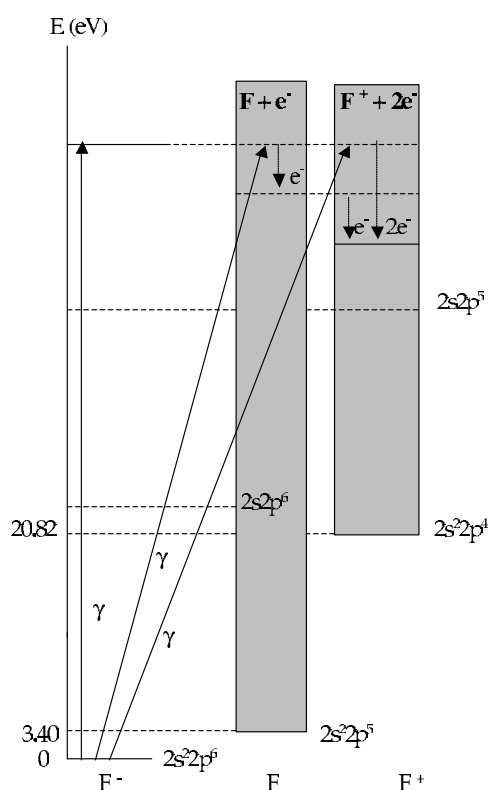
Figure 1. An energy-level diagram covering the range of photon energies used in the experiment. The figure shows resonant and non-resonant pathways from the ground state of the F^- ion into the single- and double-detachment continua. The direct non-resonant process involves the simultaneous detachment of two electrons from the 2p valence sub-shell. Indirect processes involve the sequential production and decay of an intermediate core-excited state of F arising from the detachment of a 2s electron from the F^- ion.

$2s^2 2p^6\ ^1S_0$ ground state of F^-. The symbol F^{**} represents an intermediate core-excited state (j) of the F atom that decays rapidly via the Auger process. Core-excited states of F, for example, have configurations of the type $2s2p^6$ or $2s2p^5 nl$. In principle, an F atom in a core-excited states may also make a radiative transition to a bound state of the F atom, producing neutrals that are not detected in the experiment. However, the radiative branching is expected to be very small in the present case. The $2s2p^6$ state lies just above the $2s^2 2p^5$ limit and therefore should preferentially decay by electron emission rather than photon emission. The final state (k) of the F^+ ion will be either the ground state or an excited state, depending on the photon energy. The sequential two-electron detachment process described above is shown in figure 1. Essentially, the inner-shell vacancy produced in the F^- ion in the detachment of the first electron is transferred to the F atom, leaving it in a core-excited state, which subsequently decays to the two-electron detachment continuum via an Auger process. It should be noted that a similar sequential process could also be mediated by doubly excited states of F of the type $2s^2 2p^3 nl n'l'$. In this case the process is initiated by the detachment of a single 2p valence electron, which proceeds to interact with the other electrons in the valence sub-shell as it leaves the F atom. The formation of such states would, however, involve a higher degree of electron correlation and are therefore expected to play a much smaller role in the production of F^+ ions.

In addition to the non-resonant processes mentioned above, it is possible that core-excited or multiply-excited resonant states of the F$^-$ ion could play a role in the detachment of two electrons. Such states would have, for example, configurations of the type $2s2p^6nl$, $2s2p^5nln'l'$ or $2s^22p^4nln'l'$. These highly correlated states would be embedded in both the single- and double-detachment continua. They could therefore decay by autodetachment as they couple directly to the two-electron continuum, simultaneously ejecting two valence electrons. More likely, the two excited electrons would be ejected sequentially. In this case, the resonant state of the F$^-$ ion would first autodetach by interacting with the one-electron continuum. The resulting core-excited and multiply-excited states of the F atom would then decay by Auger emission or auto-ionization, producing F$^+$ ions. No prominent resonances were observed in the experiment.

The R-matrix method has been used in this study to calculate the cross section over the range of energies covered in the experiment. This computational method was initially developed to study electron–atom scattering [20]. However, in the half-collision concept, the processes of photo-detachment and electron–atom scattering are equivalent, and so the R-matrix method has also been used effectively on many occasions to describe the process of photo-detachment. In the present calculation of the cross section for the production of F$^+$ ions from F$^-$ ions in the photo-double detachment process we employed an $n = 3$ orbital basis and used multi-configuration target wavefunctions expansions of the neutral F atom state in the scattering calculation. We used the 1s, 2s and 2p Hartree–Fock orbitals of Clementi and Roetti [21] in our work, augmented with $n = 3$ orbitals that were determined in a manner similar to the work of Baliyan and Bhatia [22]. The radial parameters associated with these $n = 3$ orbitals were determined by energy optimization using the CIV3 structure code of Hibbert [23]. The electric dipole selection rules limit the final states to ^1P_o symmetry since the ground state of F$^-$ has ^1S symmetry, therefore in the L–S coupling scheme, only doublet states of the neutral fluorine atom can couple to the outgoing continuum electron (εs, εp, $\varepsilon d \ldots$) to yield the ^1P_o scattering states. Photodetachment cross sections were determined in the L–S coupling scheme using the scattering codes developed for the International R-matrix/Opacity, Iron Project and the RmaX project [24–26].

In our calculations 36 states of the neutral fluorine atom were used. They were generated from multi-configuration interaction mixing of the following electron configurations: $2s^22p^5$, $2s^22p^43l$, $2s2p^6$, $2s2p^43l3l'$, $2s^22p^33l3l'$ $2s^22p^23l^23l'$ and $2s2p^53l$. The scattering calculations were carried out using 40 continuum orbitals, which were Lagrange orthogonalized to the bound orbitals. In the R-matrix photodetachment calculations a boundary radius of 33.4 Bohr radii was required to contain the electron density of the $n = 3$ basis and triple-electron promotions from these base configurations were used to represent the wavefunction for the scattered electron. In the outer region, electron scattering calculations from the F atom were carried out with an energy mesh sufficiently fine (approximately, 1.36 meV) in order to resolve any narrow resonance structure that might be present in the photo-double detachment cross section. In our work, the cross section for double-electron detachment was obtained by adding together the partial single-electron detachment cross sections involving the final states of neutral F that lie above the F$^+(2s^22p^4\ ^3P)$ ground state threshold. The calculated electron affinity of the F atom was found to be 3.36 eV, which is in reasonable agreement with the accepted experimental value of 3.401 90(4) eV [2]. We performed a separate (but similar) R-matrix calculation in an attempt to quantify the contribution to double detachment made by the direct process. In this 36 state calculation, the Hartree–Fock orbitals were augmented with $n = 3$ pseudo-orbitals [27]. Here again, cross sections for double detachment into states above the F$^+$ ground state were summed over. Unlike the physical $n = 3$ orbitals, the pseudo-orbitals lie in the single-electron continuum. Hence they
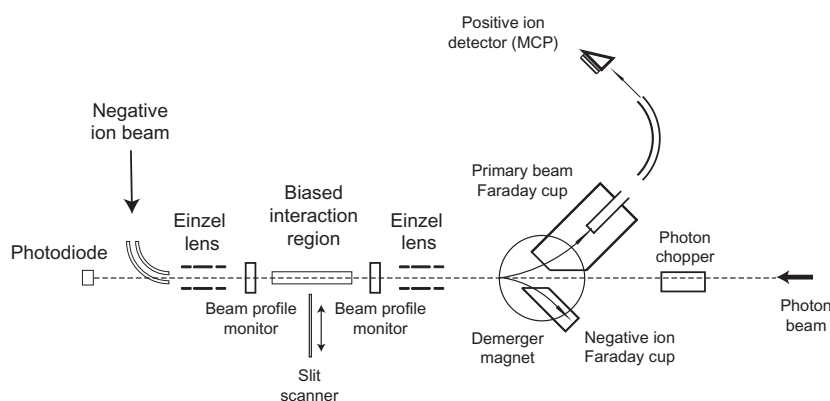
Figure 2. A schematic of the apparatus showing the counter-propagating beams of negative ions from the ion source and photons from the synchrotron source. The collinearly merged beams interact in the biased interaction region. The spatial overlap of the two beams was measured by the beam profile monitors.

can describe processes where the second ('atomic') electron is transferred directly into the continuum.

A separate random phase approximation calculation was performed in order to verify the role played by the lowest-lying, core-excited $2s2p^6$ state of F in the production of F^+ ions. This state lies above the ionization threshold of F^+ and therefore decays predominantly via Auger processes to form F^+ ions. The contribution of this intermediate state to the total F^+ production cross section has been determined by calculating the cross section for the photodetachment of a 2s electron from the F^- ion using the RPA. This calculation takes into account the correlation between the $2p \rightarrow \varepsilon s$, εd and the $2s \rightarrow \varepsilon p$ dipole transitions. The calculation shows that the strong $2p \rightarrow \varepsilon d$ transition suppresses the $2s \rightarrow \varepsilon p$ transition and noticeably modifies its energy dependence. The resulting cross section is similar to that obtained in a previous relativistic RPA calculation [19].

3. Experimental procedure

In the experiment, we used the 10.0.1 undulator beamline at the Advanced Light Source (ALS) synchrotron radiation facility situated at the Lawrence Berkeley National Laboratory. The measurement was performed at the ion–photon-beam endstation, 10.0.1.2. A schematic of the apparatus is shown in figure 2. A more detailed description of the apparatus can be found in a recent paper by Covington *et al* [28]. A beam of negative ions from a low-energy accelerator was collinearly overlapped with a beam of vuv photons from the synchrotron source. The two beams were merged in a counter-propagating geometry. The F^- ions were produced in a sputter ion source, extracted at a energy of 5 keV and focused by means of a series of cylindrical electrostatic lenses. The ion beam was then momentum selected using a $60°$ analysing magnet. The cross-sectional area of the ion beam was defined by a pair of adjustable slits mounted in a plane perpendicular to the direction of propagation of the beam. The ion beam was then merged onto the axis of the counter-propagating photon beam using a set of $90°$ spherical-sector bending plates. The primary ion beam then entered a 29.4 cm long cylindrical interaction region which was biased at +2 kV in order to energy label the F^+ ions produced as a result of the photon–ion interaction. These ions had an energy of 9 keV after they left the interaction region. The energy labelling of the F^+ ions produced by photodetachment

enabled us to distinguish them from the F^+ ions produced in double-detachment collisions of F^- ions with the residual gas along the entire unbiased region of the beam line since these ions would have an energy of 5 keV. The collisional background contribution was also reduced by maintaining a vacuum of 5×10^{-10} Torr in the beam line.

In the centre of the interaction region, the spatial overlap between the ion and photon beams was measured using a stepping-motor-driven slit scanner. Spatial overlap measurements took less than 1 min to complete, and the two beams were typically stable for much longer time periods. Rotating-wire beam-profile monitors were used just upstream and downstream of the interaction region to ensure that the two beams were well collimated over the entire interaction region. The fine tuning of the overlap of the two beams was achieved by using two sets of mutually perpendicular electrostatic steering plates mounted immediately behind the plates used to merge the ion beam onto the axis of the photon beam. This procedure allowed us to measure the beam overlap quantitatively and use it to establish an absolute scale for the cross section data. Absolute measurements of the cross section were made at eight different energies across the cross section curve. A small correction was made to the photon energy scale to account for the Doppler shift associated with the moving ions.

After the interaction region, a $45°$ analysing magnet was used to separate the energy-labelled positive ions produced by photodetachment in the interaction region from the primary negative ion beam and the positive ions produced in collisional detachment. The photo-ions had an energy of 9 keV, whereas most of the positive ions produced in collisions with the residual gas had an energy of 5 keV, as determined by the extraction voltage at the ion source. The photon beam was modulated at a frequency of 6 Hz using a computer-controlled shutter in order to discriminate against the small collisionally induced background of 9 keV positive ions created in the interaction region. The 9 keV photo-ions were further deflected, in the vertical dispersion plane, by use of a set of $90°$ spherical-sector bending plates. This was done to minimize any background arising from the collection of the primary negative ion beam. The dispersed F^+ photo-ions then entered a negatively biased box surrounding the detector. Inside the box, the ions struck a metal plate and produced secondary electrons. These secondary electrons were accelerated toward a micro-channel plate detector operating with a positively biased anode (~ 300 V). The ion detection efficiency was measured by passing a very small intensity ion beam through the apparatus, and measuring the current on the metal plate with a sub-femto-ampere current metre. The current measurement is compared to the count rate from the secondary electrons detected with the micro-channel plate detector to determine the detection efficiency. The efficiency for the detection of the F^+ ions was estimated to be 0.62(9). The pulses generated by the electrons were amplified and passed through a single-channel analyser to discriminate against electronic noise. The output of the discriminator was converted to transistor–transistor logic pulses and counted with an input/output board in a PC-based data acquisition and control system. Typically, the F^- ion beam current in the interaction region was of the order of a 100 nA. The magnitude of this current was monitored and used to normalize the yield of photo-ions. Similarly, the photon intensity was monitored for normalization purposes using a calibrated Si p–n junction photodiode [29]. The analogue outputs of the monitors of the ion beam and photon beam intensities were digitized and counted. The normalized photo-ion signal is inversely proportional to the double-detachment cross section.

4. Results

The relative cross section measurements for the photo-double detachment from the F^- ion over the energy range 20–62 eV are shown in figure 3. The cross section scale was established by
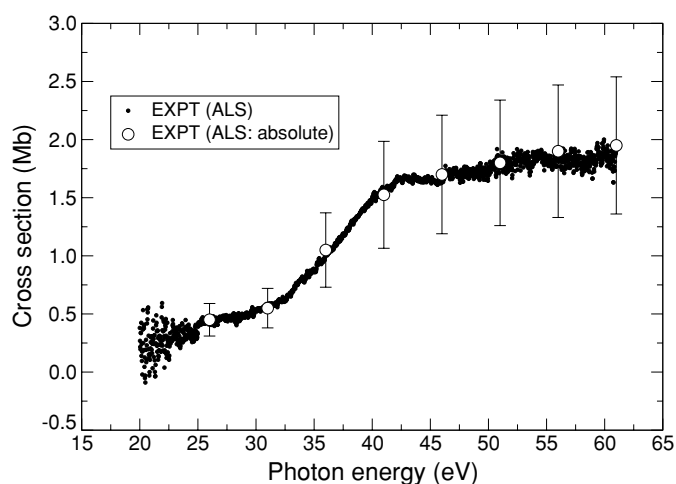
Figure 3. The measured cross section for the production of F^+ ions from F^- ions in a photo-double detachment process. The cross section scale was established by making absolute measurements (denoted by the open circles) at the eight energies shown. The photon energy scale is measured relative to the ground state of F^-. The increased statistical scatter in the data below 25 eV and above 46 eV is due to smaller accumulation times.

making a series of eight absolute measurements. In the figure, these data points are indicated by the open circles. The error bars on the absolute data points represent the systematic uncertainties in the measurements. These are estimated to be about 35%. The dominant contributions to the estimated uncertainty are the beam overlap integral, 14%, the beam profile measurement, 9%, photodiode responsivity, 7% and photo-ion signal counting statistics, 4%. It is interesting to note that the overall magnitude of the photo-double detachment cross sections for F^- is similar to that measured for Cl^- [13]. However, the latter cross section displayed a more rapid variation with the photon energy.

In figure 4, a comparison is made between the eight data points representing the measured absolute cross sections and cross sections predicted by the *R*-matrix and RPA calculations. First, note that the RPA and *R*-matrix calculations for the $2s2p^6$ state of F are similar in shape and the cross sections are much smaller than the measured cross section. This is in contrast to the Cl^- case, where the 3s detachment cross section obtained by the RPA calculation [19] was much higher (although still below the experimental cross section). Note also that there is an interesting difference between the role of the $3s \rightarrow \varepsilon p$ photodetachment channel in Cl^- and that of the $2s \rightarrow \varepsilon p$ channel in F^-. This difference is related to the nature and energy of the $nsnp^6\,^2S$ states in Cl ($n = 3$) and F ($n = 2$). The NIST data tables [30] identify only one level at 10.623 eV above the Cl ground state, which contains 49% of the $3s3p^6$ configuration. This level lies below the Cl^+ threshold, hence it cannot contribute to double-electron detachment. However, it appears that the $3s3p^6$ configuration is strongly mixed, in particular, with the $3s^23p^43d$ configuration. As a result, some of the eigenstates of Cl that lie above the Cl^+ threshold ($3s3p^6$ satellites) and which contain sizeable contribution from the $3s3p^6$ configuration, can autoionize to yield Cl^+ ions. Similar satellites in the iso-electronic Ar atom have been studied extensively. The paper by Kossmann *et al* [31] is an example of this work. Therefore, only a fraction of the $3s \rightarrow \varepsilon p$ cross section predicted by the RPA calculation [19] may contribute to the production of Cl^+ ions. In contrast, the situation in the case of F appears to be simpler, since the $2s2p^6$ state lies 3.63 eV above the F^+ threshold [30]
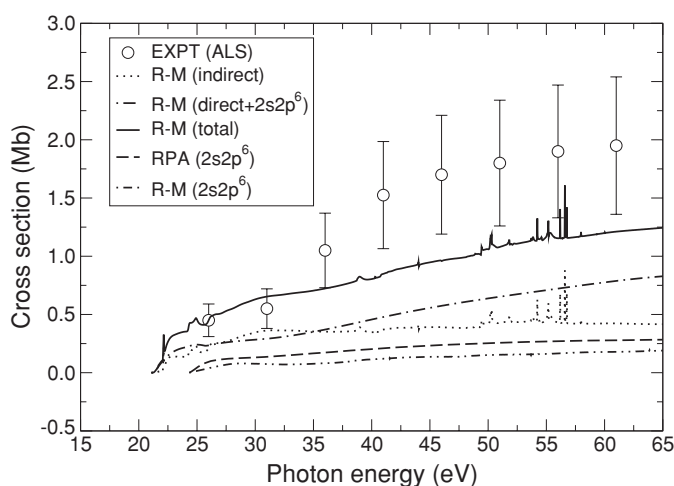
Figure 4. Cross sections for the production of F^+ ions from F^- ions via the process of photo-double detachment. The eight data points represented by open circles are absolute measurements. The photon energy scale is relative to the ground state of the F^- ion. The representations of the various calculations are shown in the inset. R-M refers to R-matrix calculations.

and does not mix strongly with other configurations. Hence, the $2s \rightarrow \varepsilon p$ photodetachment process lead primarily to the production of F^+ ions via the Auger effect. The RPA calculations indicate, however, that its contribution is not large.

Figure 4 also shows the R-matrix calculations obtained with physical and pseudo-states. Since these two calculations represent essentially different mechanisms of formation of F^+ ions, we also show their sum. This sum accounts for the formation of F^+ via intermediate core-excited states (and possibly autoionizing satellite states) of F and for the direct promotion of the second electron into the continuum. The overall shape of the calculated R-matrix cross section is in reasonable agreement with the measured cross section. The energy dependences of the calculated cross sections for the direct and indirect processes differ above 40 eV. One can see that the rise of the measured cross section better matches the energy dependence of the calculated cross section obtained using pseudo-states, while its near-threshold behaviour seems closer to that obtained using the physical states. This may be an indication that the simultaneous removal of two electrons becomes dominant at higher photon energies, above 40 eV.

We attribute the observed discrepancy in magnitude between the experimental and theoretical cross sections to the limited size of the basis set used in our calculations. In particular, the representation of the continuum is limited by the $n = 3$ pseudo states. One would ideally need to perform large scale R-matrix plus pseudo states (RMPS) calculations that would include the physical $n = 3$ states and states derived from the use of $4l, 5l, 6l \ldots$ pseudo-orbitals to adequately represent the continuum. The measured cross section is systematically higher than the calculated cross section above about 40 eV, although this may not be too significant given the combined uncertainties in both measurement and calculation. Overall, the calculations support an understanding that the direct mechanism of the detachment of a pair of 2p electrons dominates the double-detachment cross section in the case of F^-, at least at energies well above the threshold region. In the case of F^-, this dominance may simply be due to the fact that the 2p sub-shell is very tightly bound and the electrons consequently interact strongly with each other.

5. Summary

We have measured the cross section for photo-double detachment leading to the production of F^+ ions from F^- ions. The relative cross sections were measured over the range 20–62 eV. In addition, eight absolute measurements were made to establish a cross section scale. *R*-matrix and RPA calculations were performed in an attempt to understand the mechanisms responsible for double detachment from F^-. Resonant processes did not appear to play a significant role. Two non-resonant processes were identified as mechanisms for producing F^+ ions from F^- ions. In the direct process a pair of 2p electrons from the valence sub-shell are simultaneously detached from the negative ion. The primary competing indirect process is sequential and is initiated by the detachment of a 2s electron, which results in the production of intermediate core-excited states of the neutral F atom. The core-excited states of F subsequently decay via Auger emission producing F^+ ions. Both the RPA and the *R*-matrix calculations indicate that this process makes a very small contribution to the total double-electron detachment cross section. The calculations show that the dominant mechanism for the production of F^+ ions from F^- ions at energies well above threshold is the direct process. It is interesting to note that while the double-electron detachment cross sections for F^- and Cl^- have similar overall magnitudes, their dependence on photon energy is very different. The cross section for Cl^- peaks close to threshold (at about 25 eV), and then drops off relatively rapidly. The cross section for F^-, on the other hand, continues to rise from threshold to 60 eV, the highest energy used in the measurement. This difference might be related to a much more tightly structured $2p^6$ sub-shell in F^- compared to the $3p^6$ sub-shell in Cl^-. It appears that the cross sections for double detachment from both F^- and Cl^- ions are dominated by the direct process well above threshold, this being the case more for F^- than Cl^-. The tighter structure of the 2s and 2p sub-shell in F^- relative to the 3s and 3p sub-shell in Cl^- appears to suppress the indirect process involving core detachment and enhance the direct process involving the correlated ejection of a pair of valence electrons.

Multiple-electron detachment following the absorption of a single high-energy photon is a process that can yield important information on the role played by electron correlation in the structure and dynamics of negative ions. In general, it appears that negative ions are well suited for such studies since energy exchanges in these loosely bound systems are smaller and as a result, higher-order process such as multiple detachment becomes more probable.

References

[1] Pegg D J 2004 *Rep. Prog. Phys.* **67** 857
[2] Blondel C, Delsart C and Goldfarb F 2001 *J. Phys. B: At. Mol. Opt. Phys.* **34** L281

[3]   Donahue J B, Gram P A M, Hynes V M, Hamm R W, Frost C A, Bryant H C, Butterfield K B, Clark D A and
        Smith W W 1982 *Phys. Rev. Lett.* **48** 1538

[4]   Bae J K, Coggiola M J and Peterson J R 1983 *Phys. Rev.* A **28** 3378

[5]   Bae J K and Peterson J R 1988 *Phys. Rev.* A **37** 3254

[6]   Kjeldsen H, Andersen P, Folkmann F, Christensen B and Andersen T 2001 *J. Phys. B: At. Mol. Opt. Phys.* **34**
        L353

[7]   Berrah N *et al* 2001 *Phys. Rev. Lett.* **87** 253002

[8]   Berrah N, Bozek J D, Turri G, Akerman G, Rude B, Zhou H-L and Manson S T 2002 *Phys. Rev. Lett.* **88** 093001

[9]   Gibson N D, Walter C W, Zatsarinny O, Gorczyca T W, Akerman G D, Bozek J D, Martins M, McLaughlin B M
        and Berrah N 2003 *Phys. Rev.* A **67** 030703(R)

[10] Bilodeau R, Bozek J D, Aguilar A, Ackerman G D, Turri G and Berrah N 2004 *Phys. Rev. Lett.* **93** 193001

[11] Berrah N, Bilodeau R C, Ackermann G, Bozek J D, Turri G, Rude B, Gibson N D, Walter C W and Aguilar A
        2004 *Phys. Scr.* **T110** 51

[12] Covington A M *et al* 2001 *J. Phys. B: At. Mol. Opt. Phys.* **34** L735

[13] Aguilar A *et al* 2004 *Phys. Rev.* A **69** 022711

[14] Zhou H-L, Manson S T, VoKy L, Feautrier N and Hibbert A 2001 *Phys. Rev. Lett.* **87** 023001

[15] Zhou H L, Manson S T, VoKy L, Hibbert A and Feautrier N 2001 *Phys. Rev.* A **64** 012714

[16] Zatsarinny O, Gorczyca T W and Fischer C F 2002 *J. Phys. B: At. Mol. Opt. Phys.* **35** 4161

[17] Carlin N M, Ramsbottom C A, Bell K L and Hibbert A 2003 *J. Phys. B: At. Mol. Opt. Phys.* **36** 3637
        Carlin N M, Ramsbottom C A, Bell K L and Hibbert A 2004 *J. Phys. B: At. Mol. Opt. Phys.* **37** 953
        Carlin N M, Ramsbottom C A, Bell K L and Hibbert A 2004 *J. Phys. B: At. Mol. Opt. Phys.* **37** 1083

[18] Amusia M Y, Gribakin G F, Ivanov V K and Chernysheva L V 1986 *Izv Akad Nauk SSSR, Ser Fiz* **50** 1274

[19] Radojevic V, Kelly H P and Johnson W R 1987 *Phys. Rev.* A **35** 2117

[20] Burke P G and Berrington K A (ed) 1993 *Atomic and Molecular Processes: an R-matrix Approach* (Bristol:
        IOP Publishing)

[21] Clementi E and Roetti C 1974 *At. Data Nucl. Data Tables* **14** 177

[22] Baliyan K S and Bhatia A K 1994 *Phys. Rev.* A **50** 2981

[23] Hibbert A 1975 *Comput. Phys. Commun.* **9** 141

[24] Seaton M J 1987 *J. Phys. B: At. Mol. Opt. Phys.* **20** 6363

[25] Berrington K A, Eissner W B and Norrington P H 1995 *Comput. Phys. Commun.* **92** 290

[26] Available on line: http://amdpp.phys.strath.ac.uk/UK RmaX.

[27] Hibbert A, LeDourneuf M and Vo Ky L 1977 *J. Phys. B: At. Mol. Opt. Phys.* **10** 1015

[28] Covington A M *et al* 2002 *Phys. Rev.* A **66** 062710

[29] Gullickson E M, Korde R, Canfield L R and Vest R E 1996 *J. Electron Spectrosc. Relat. Phenom.* **80** 313

[30] NIST Atomic Spectra Database, http://physics.nist.gov/cgi-bin/AtData/main_asd

[31] Kossmann H, Krässig B, Schmidt V and Hansen J E 1987 *Phys. Rev. Lett.* **58** 1620